Molecular Therapy
Oncolytics
Original Article

Pan-cancer analysis reveals distinct clinical, genomic, and immunological features of the *LILRB* immune checkpoint family in acute myeloid leukemia

Zi-jun Xu,[1,2,3,6] Xin-long Zhang,[4,6] Ye Jin,[2,5,6] Shi-sen Wang,[2,5] Yu Gu,[2,5] Ji-chun Ma,[1,2,3] Xiang-mei Wen,[1,2,3] Jia-yan Leng,[2,5] Zhen-wei Mao,[3] Jiang Lin,[1,2,3] and Jun Qian[2,5]

[1]Laboratory Center, Affiliated People's Hospital of Jiangsu University, Zhenjiang 212002, Jiangsu, P.R. China; [2]Zhenjiang Clinical Research Center of Hematology, Zhenjiang 212002, Jiangsu, P.R. China; [3]The Key Lab of Precision Diagnosis and Treatment in Hematologic Malignancies of Zhenjiang City, Zhenjiang 212002, Jiangsu, P.R. China; [4]Department of Hematology, The People's Hospital of Danyang, Affiliated Danyang Hospital of Nantong University, Danyang 212300, Jiangsu, P.R. China; [5]Department of Hematology, Affiliated People's Hospital of Jiangsu University, Zhenjiang 212002, Jiangsu, P.R. China

Leukocyte immunoglobulin (Ig)-like receptor Bs (*LILRB*s), a family of type I transmembrane glycoproteins, are known to inhibit immune activation. Here, we comprehensively evaluated the molecular, prognostic, and immunological characteristics of *LILRB* members in a broad spectrum of cancer types, focusing on their roles in acute myeloid leukemia (AML). We showed that *LILRB*s were significantly dysregulated in a number of cancers and were associated with immune-inhibitory phenotypes. Clinically, high expression of *LILRB1-LILRB4* predicted poor survival in six independent AML cohorts. Genetically, *LILRB1* was associated with more mutational events than other *LILRB* members, and multiple genes involved in immune activation were deleted in *LILRB1*^{high} patients. Epigenetically, *LILRB4* was significantly hypomethylated and marked by MLL-associated histone modifications in AML. Immunologically, *LILRB*s were positively associated with monocytic cells, including M2 macrophages, but were negatively associated with tumor-suppressive CD8 T cells. Importantly, patients with higher *LILRB* expression generally showed a better response to immune checkpoint blockade (ICB) in five independent immunotherapy cohorts. Our findings reveal critical immunological and clinical implications of *LILRB*s in AML and indicate that *LILRB*s may represent promising targets for immunotherapy of AML.

INTRODUCTION

Acute myeloid leukemia (AML) is a highly fatal hematopoietic malignancy marked by various cytogenetic and molecular abnormalities and variable responses to treatment.[1–3] Currently, the mainstay of treatment for AML is cytotoxic chemotherapy,[4] yet chemoresistance and relapse are commonly seen in clinical practice. Some novel regimens, such as hypomethylating agents (HMAs), Bcl-2 inhibitors, Fms-like tyrosine kinase 3 (*FLT3*), and isocitrate dehydrogenase (*IDH*) inhibition, have shown promising results in certain subsets of patients with AML.[5,6] Since 2017, the US Food and Drug Administration (FDA) has approved some new agents, such as enasidenib for patients with relapsed/refractory *IDH2*-mutated AML, gilteritinib for *FLT3*-mutated AML, and liposomal cytarabine-daunorubicin CPX-351 for therapy- and myelodysplastic syndrome (MDS)-related AML.[7] However, there still remains an urgent need to develop novel effective therapies for various subsets of AML.

Of note, immune checkpoint inhibitors (e.g., anti-*PD-1* and anti-*PD-L1* antibodies) have revolutionized cancer treatment during the past decade in treating cancers such as non-small cell lung carcinoma and melanoma;[8] however, the transfer of immunotherapy to AML has been less successful than to other cancers.[9] Indeed, the AML microenvironment is predominantly immunosuppressive. For example, we have previously demonstrated that M2 macrophages, a classical immunosuppressive component, were preferentially enriched in AML than other hematological malignancies and normal controls.[10] Also, a recent single-cell RNA sequencing (RNA-seq) study has identified proportionally fewer T cells and cytotoxic T lymphocytes (CTLs) in AML than normal controls, and the function of these T cells is profoundly impaired, probably mediated by CD14+ monocyte-like cells.[11,12] Moreover, Noviello et al. found that bone marrow (BM) T cells at AML relapse showed an exhausted phenotype, which was absent in patients maintaining long-term complete response.[13] These findings suggest encouraging therapeutic opportunities by modulating the immune environment in AML.

Received 21 December 2021; accepted 27 May 2022;
https://doi.org/10.1016/j.omto.2022.05.011.

[6]These authors contributed equally

Correspondence: Jun Qian, Prof., Department of Hematology, Affiliated People's Hospital of Jiangsu University, 8 Dianli Rd., 212002 Zhenjiang, P.R. China.
E-mail: qianjun0007@hotmail.com
Correspondence: Jiang Lin, Prof., Laboratory Center, Affiliated People's Hospital of Jiangsu University, 8 Dianli Rd., 212002 Zhenjiang, P.R. China.
E-mail: 2651329493@qq.com
Correspondence: Zhen-wei Mao, Prof., The Key Lab of Precision Diagnosis and Treatment in Hematologic Malignancies of Zhenjiang City, Affiliated People's Hospital of Jiangsu University, 8 Dianli Rd., 212002 Zhenjiang, P.R. China.
E-mail: maopen365@163.com

Leukocyte immunoglobulin (Ig)-like receptor subfamily B (*LILRB*) proteins are a group of type I transmembrane glycoproteins with extracellular Ig-like domains that bind ligands and intracellular immunoreceptor tyrosine-based inhibitory motifs (ITIMs).[14] This group of receptors contains 5 members (*LILRB1–LILRB5*) mainly expressed in hematopoietic cells and also various types of tumors.[14] As these proteins negatively regulate immune activation,[15–17] they are often considered as immunosuppressive components in the tumor microenvironment (TME). In AML, the TME-modulating role of *LILRB*s has recently come into focus, especially for *LILRB4*. Gui et al. demonstrated that *LILRB4* facilitates tissue infiltration of AML cells by substantially suppressing T cell activities, while blocking *LILRB4* activity efficiently inhibited AML development *in vitro* and *in vivo*.[18,19] In addition, *LILRB1* was found to be more highly expressed in dysfunctional CD8+ T cells from AML than T cells from healthy controls.[20] Interestingly, a non-immunological AML-promoting role was reported for *LILRB2*, which binds *ANGPLT2* to maintain stemness of normal stem cells and support leukemia development by inhibiting differentiation of AML cells.[21] Despite the functional importance of *LILRB*s in AML, there lacked a systematic study to explore the expression patterns, clinical implications, and immunological features of all *LILRB* members in AML. Therefore, in this study, drawing on rich multi-omics data in the public domain, we comprehensively evaluated the transcriptional levels and prognostic significances of *LILRB* members in a broad spectrum of cancer types, focusing on its role in AML. In addition, we systematically characterized the genomic and immune landscape in patients with AML with altered *LILRB* expression.

RESULTS

Landscape of genetic and expression alterations of *LILRB*s across cancer types

We first determined the expression patterns of *LILRB*s in different human tissues based on reads per kilobase of transcript per million mapped reads (RPKM) values using Genotype-Tissue Expression (GTEx; http://www.GTExportal.org/home/).[22] We observe that *LILIB*s were highest expressed in the spleen, followed by blood and the lung tissue, while weakly expressed in other tissues (Figure S1). Importantly, the preferential enrichment of *LILRB*s in spleen was further validated in the FANTOM5 and Human Protein Atlas (HPA) dataset (Figures S2 and S3). Next, using Cancer Cell Line Encyclopedia (CCLE), we showed that *LILRB*s were relatively highly expressed in malignant hematological cell lines from AML, acute lymphocytic leukemia (ALL), lymphomas, and multiple myeloma (MM) (Figure S4). Moreover, we observed a strong protein expression of *LILRB1–LILRB4* in monocytes via Human Proteome Map (https://www.humanproteomemap.org/) (Figure S5). Together, these findings indicated cellular-, tissue-, and disease-specific *LILRB* expression. Combining the normal tissue of the GTEx dataset as controls, we then systematically compared *LILRB* expression between tumor and adjacent normal tissue across 28 cancer types (9,465 tumor and 7,831 normal samples). Surprisingly, *LILRB*s were significantly dysregulated in almost all cancer types (Figures 1A and S6). For *LILRB1*, *LILRB2*, and *LILRB4*, increased expression in tumors was more commonly seen, whereas *LILRB3* and *LILRB5* were significantly down-regulated in the majority of cancer types (Figures 1A and 1B). For *LILRB1–LILRB4*, the most remarkable difference was observed between AML and normal counterparts (Figures 1A and S6). We also investigated genetic alteration (including mutations, amplifications, and deletions) frequencies of *LILRB*s across pan-cancers. The average alteration frequencies of five genes are summarized in Figure S7, and the oncoprint is present in Figure S8A. The highest mutation loads of *LILRB*s were observed in skin cutaneous melanoma (SKCM) (Figure 1C). Overall, *LILRB1* was the most highly mutated and *LILRB3* the least; the most frequent genomic variants were missense mutations for five genes (Figures 1D and S8B). Amplifications were more commonly seen in cancers such as adrenocortical carcinoma (ACC) and uterine carcinosarcoma (UCS), while deletions were mostly found in brain lower grade glioma (LGG) (Figures 1E and S7). By analyzing the methylome data of *LILRB*s across 30 cancer types with matched controls through the human disease methylation database Diseasemeth v.2.0 (http://bio-bigdata.hrbmu.edu.cn/diseasemeth/), we found that *LILRB* members were significantly hypomethylated in almost all cancer types analyzed compared with normal samples (Figure 1F). Furthermore, the level of methylation was negatively associated with the level of mRNA expression in most cancer types (Figure S9A). Analyzing the relation between methylation and survival revealed that hypomethylation of *LILRB*s predicted worse survival in most cancers (Figure S9B). Finally, Cox regression analyses were used to explore the association between *LILRB* expression and overall survival (OS) in TCGA pan-cancer datasets. Overall, we found that the significance and direction of the prognostic significances varied, depending on the cancer types analyzed. For example, increased expression of *LILRB* family members was generally associated with worse OS in kidney renal clear cell carcinoma (KIRC), LAML, LGG, thymoma (THYM), and uveal melanoma (UVM), while in SKCM, the reverse was observed (Figure 1G).

Association between *LILRB* expression and immune responses in cancers

LILRB family genes have been known for their immune inhibitory functions in cancers. For example, *LILRB4* has been shown to suppress T cell activation and support tissue infiltration of AML cells.[18] We hypothesized that they might be associated with specific immunologic programs in cancers. Previously, Thorsson et al. have identified six immune subtypes across cancers: C1 (wound healing), C2 (INF-r dominant), C3 (inflammatory), C4 (lymphocyte depleted), C5 (immunologically quiet), and C6 (tumor growth factor beta [TGF-β] dominant).[23] We found that all *LILRB* members exhibit the highest expression in C6 (Figure 2A), a highly immunosuppressive subtype displaying increased M2 macrophage infiltration, and conferred the worst prognosis in respective tumors. Recent research has developed four distinct TME subtypes conserved across a broad array of cancers: (1) immune enriched, fibrotic (IE/F), (2) immune enriched, non-fibrotic (IE), (3) fibrotic (F), and (4) immune depleted (D).[24] We found that patients with high *LILRB* expression possessed primarily subtypes IE/F and IE, whereas patients with low *LILRB* expression were mainly concentrated in the D subtype (Figure 2B). Next, we investigated the association between *LILRB*s and 29 TME signature scores calculated using TCGA pan-cancer data.[24] We observed strong

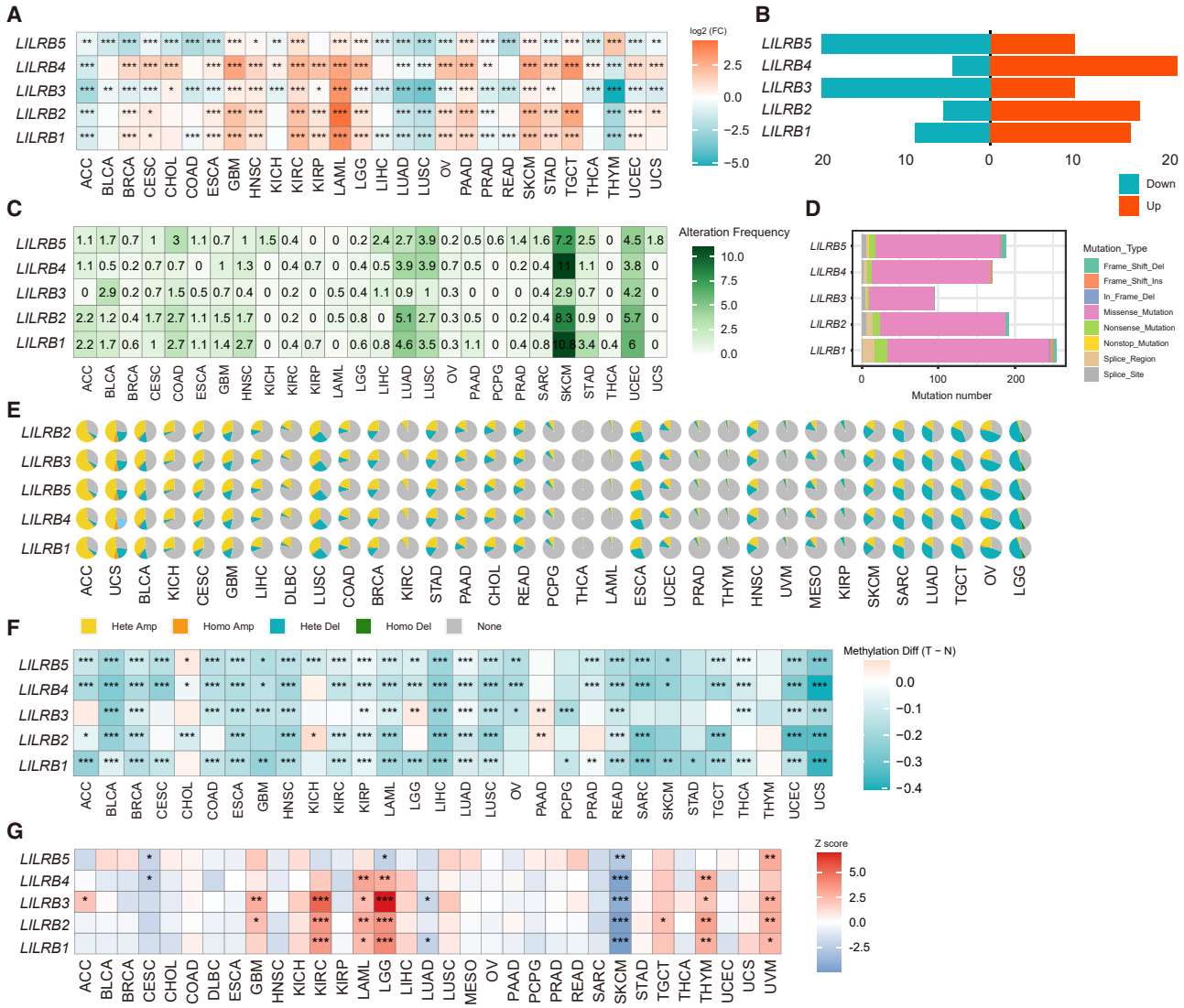

Figure 1. Landscape of genetic and expression alterations of *LILRB*s across cancer types

(A) Heatmap of differential expression profiles of *LILRB*s between tumor and normal tissue samples, combining data from TCGA and GTEx databases. The color depicts the log2-transformed fold change (Log2FC) between tumor and normal tissues. (B) Bar plot showing genes significantly up- and down-regulated ($p < 0.05$) across different cancer types. Red, up-regulated expression; blue, down-regulated expression. (C) Heatmap showing mutation frequencies of *LILRB*s across different cancer types. Numbers on the cells represent mutation percentages. (D) Bar plot showing the percentages of various mutation types for five *LILRB* genes. (E) Pie plots showing the percentages of various copy-number alteration (CNA) types for five *LILRB* genes. (F) Heatmap of differential methylation profiles of *LILRB*s between tumor and normal samples, using data from the Diseasemeth database. The color depicts methylation differences between tumor (T) and normal (N) tissues. (G) Association between *LILRB* expression and patient prognosis across 33 cancer types as determined by the Cox regression model. *$p < 0.05$; **$p < 0.01$; ***$p < 0.001$. See also Figures S1–S9.

positive correlations between *LILRB* expression with both anti-tumor and tumor-promoting immune processes (especially checkpoint inhibition) but weak correlations with stromal components and cancer cell properties (Figure 2C).

Validation of the prognostic significance of *LILRB*s in AML

Our data, along with previous studies, reflect an AML-specific expression pattern of *LILRB*s.[18,19] In this study, we focus on *LILRB*s in AML. Cox analyses in TCGA data showed that *LILRB1–LILRB4* negatively impact the survival of patients with AML. It is of particular interest to validate the prognostic value of *LILRB*s using Kaplan-Meier methods in larger patient cohorts of AML. To this end, we collected five independent datasets from GEO; X-tile was used to determine the optimal thresholds for each *LILRB* member in TCGA and GEO datasets. First, we were able to validate the adverse prognostic impact for *LILRB1–LILRB4* in the TCGA cohorts, whereas high *LILRB5* was associated with a favorable outcome (Figure S10). Importantly, the prognostic value of *LILRB1–LILRB4* also extended to the event-free

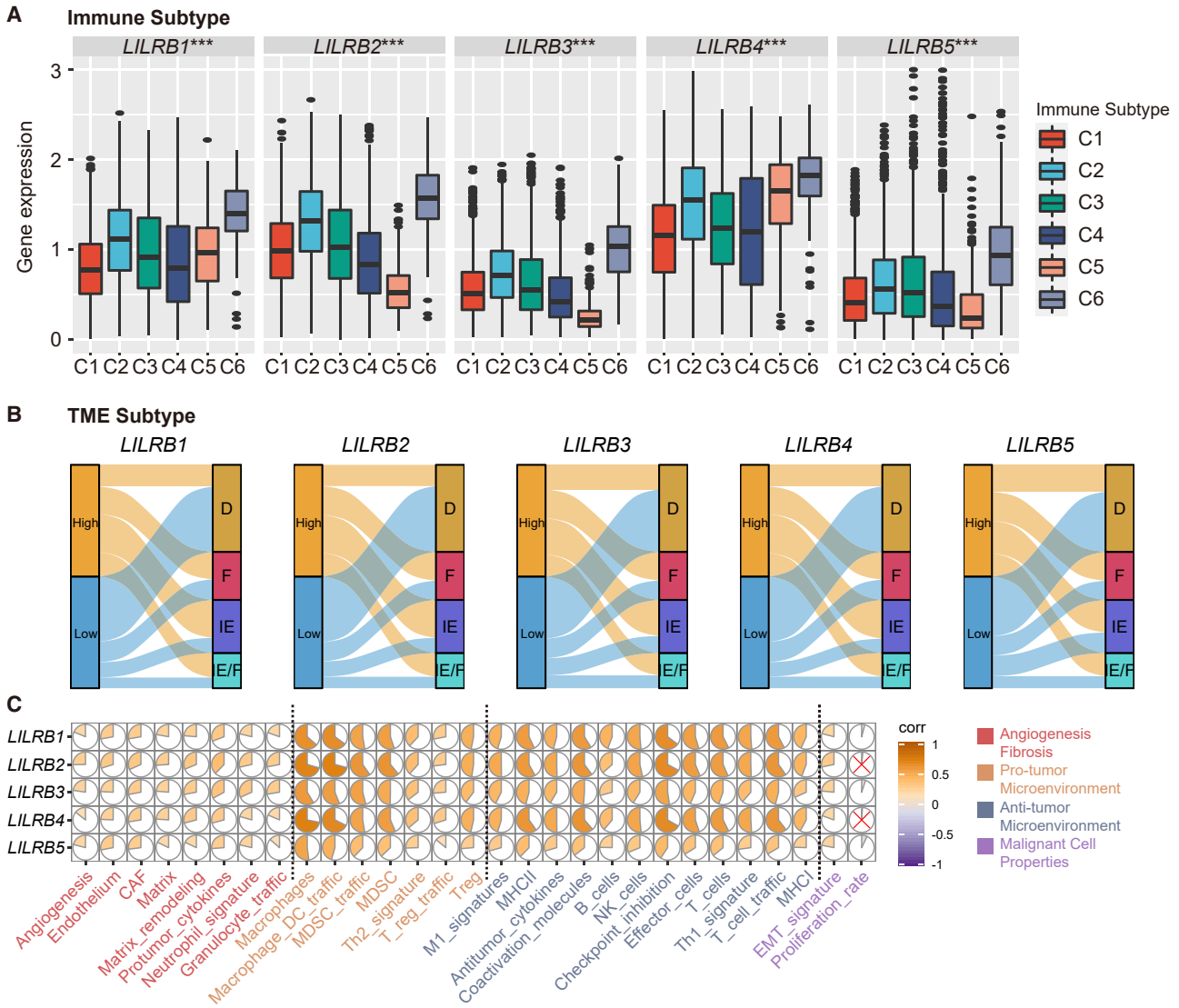

Figure 2. Association of *LILRB* family gene expression with tumor microenvironment factors

(A) The expressions of *LILRB*s within different immune infiltrate subtypes across pan-cancers tested with ANOVA. C1: wound healing, C2: INF-r dominant, C3: inflammatory, C4: lymphocyte depleted, C5: immunologically quiet, and C6: TGF-β-dominant.(B) Sankey diagram showing the links between *LILRB* expression and TME subtypes across pan-cancers. IE/F, immune-enriched, fibrotic; IE, immune-enriched, non-fibrotic; F, fibrotic; D, immune-depleted. *LILRB* expression statuses were stratified by the median expression value of respective genes. (C) Correlation matrix plots showing the association between expressions of *LILRB*s and 29 TME signature scores calculated using TCGA pan-cancer data. Spearman correlation was used for testing.

survival (EFS) endpoint and cytogenetically normal (CN) AML subsets (Figures S11A–S11C). Furthermore, the adverse prognostic impact of *LILRB*s was validated in TCGA microarray data (n = 183) (Figure S11D) and five other independent cohorts of patients with AML (GEO: GSE10358, n = 304; GSE37642 [U133A], n = 422; GSE37642 [U133plus2], n = 140; GSE106291, n = 250; GSE71014, n = 104) (Figures 3A–3E and S12A), although in some cases, only a trend for shorter OS was observed. However, *LILRB5* showed opposite prognostic effects in the GEO: GSE37642 (U133A) and GSE71014 datasets compared with that of TCGA, and no statistically significant associations were detected in the other three datasets (Figures S12A and S12B).

LILRB expression correlates with distinct genomic alterations in AML

We then examined the associations between *LILRB* expression and the clinical and genetic characteristics in the TCGA AML cohort. We found an association between *LILRB* expression and the French-American-British (FAB) classification of AML: a higher percentage of myelomonocytic or monocytic morphology (M4/M5

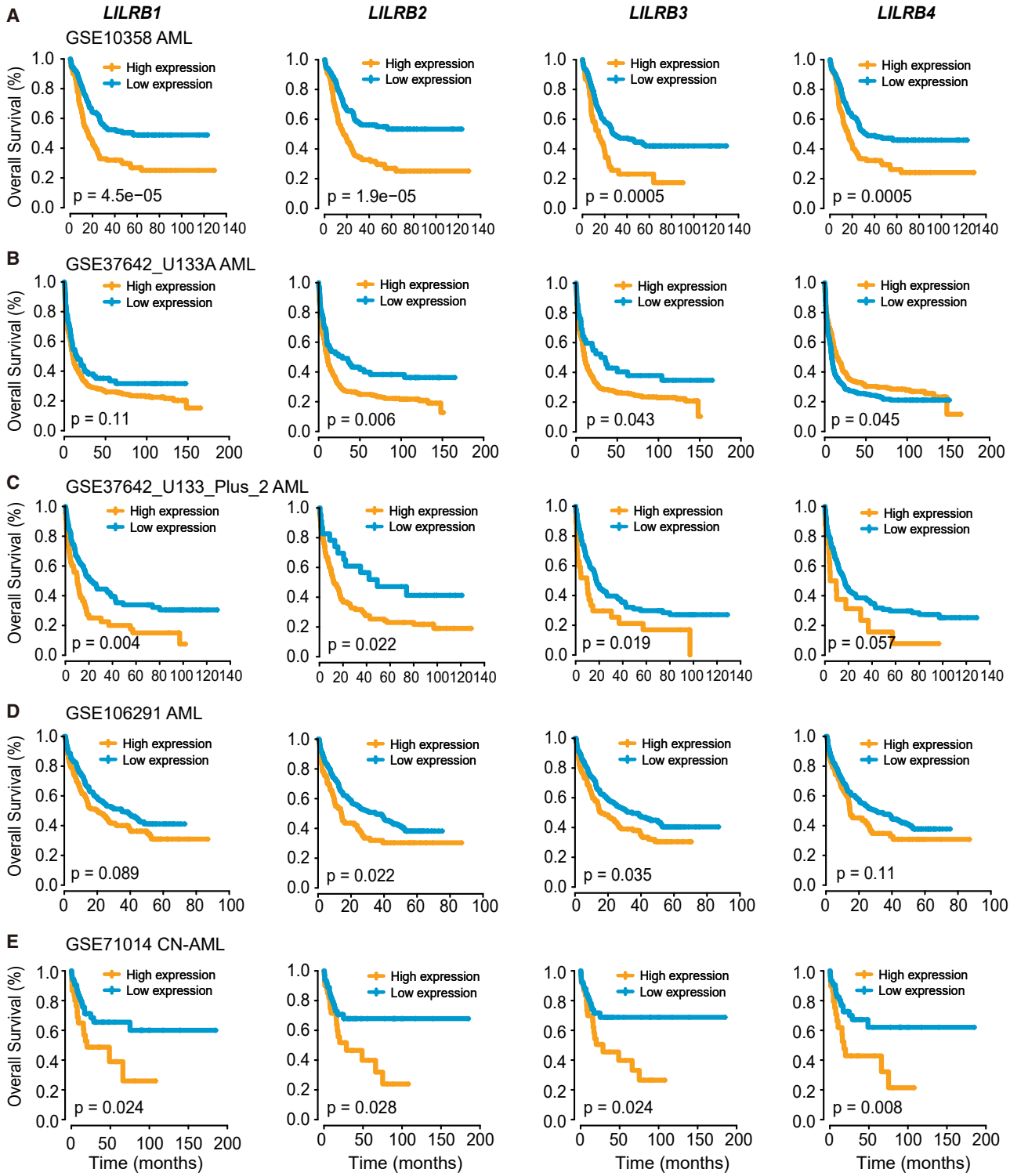

Figure 3. Independent validation of the prognostic significance of *LILRB*s in five GEO datasets

(A–E) Kaplan-Meier curves representing OS of five AML cohorts from GEO (GEO: GSE10358, n = 304; GSE37642 [U133A], n = 422; GSE37642 [U133plus2], n = 140; GSE106291, n = 250; GSE71014, n = 104) based on the expression of indicated *LILRB* members (*LILRB1–LILRB4*). The optimal cutoff of each gene was determined by the X-tile method. See also Figures S10–S12.

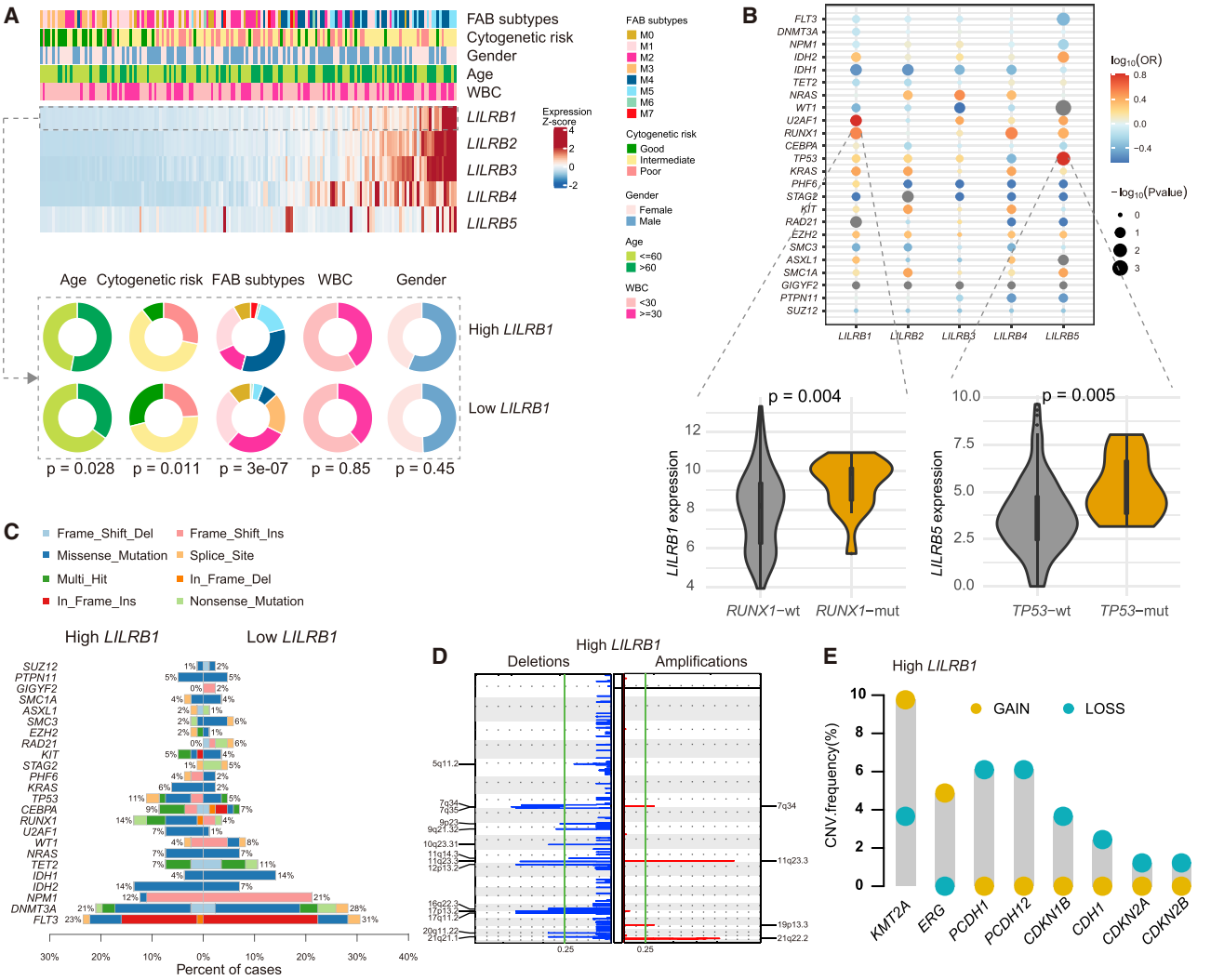

Figure 4. *LILRB* expression correlates with distinct genomic alterations in AML

(A) Heatmap showing association between *LILRB* expression and clinical characteristics in the TCGA AML cohort (top panel). Pie charts showing the chi-squared test of clinicopathologic factors for *LILRB1* status using the median expression as the cut off (bottom panel). (B) Bubble plot showing associations between the expression of *LILRB1–LILRB5* (as stratified by the median expression value of respective genes) and common mutational events in the TCGA dataset (top panel). Bubble size indicates -log10 (Fisher test p value). Color signifies log10 (odds ratio [OR]), positive association is indicated with red circles, negative with blue circles, and non-association with gray circles. *LILRB1* expression stratified by *RUNX1* mutation status, and *LILRB5* expression stratified by *TP53* mutation status (bottom panel). (C) Co-bar plots showing the comparison of mutational profiles between patients with high and low *LILRB1* expression (as stratified by the median expression value) in the TCGA dataset. (D) GISTIC analyses identified recurrent CNAs in patients with AML with high *LILRB1* expression. (E) The CNV variation frequency of indicated oncogenes and tumor-suppressor genes in patients with AML with high *LILRB1* expression. The height of the column represented the alteration frequency. Yellow dot indicates the amplification frequency; blue dot indicates the deletion frequency. See also Figure S13.

subtypes) and a lower percentage of FAB M2/M3 were observed in patients with high *LILRB* expression (Figure 4A). Moreover, high *LILRB* expressers were more likely to be >60 years old and less likely to present with favorable cytogenetics (Figure 4A).

We hypothesized that altered *LILRB* expression would have an impact on the mutation landscape of AML patients. To determine whether *LILRB1–LILRB5* correlated with distinct mutational profiles characterized for AML, we identified significantly mutated genes that occurred in patients with high and low *LILRB1–LILRB4* expression (as stratified by the median expression value of respective genes) using curated mutational data from TCGA. Overall, we found *LILRB1* and *LILRB5* expression was associated with more mutational events than the other three genes (Figure 4B). As shown in Figure 4C, patients with high *LILRB1* expression had a higher frequency of mutations in *U2AF1* (7% versus 1%) and *RUNX1* (14% versus 4%), while *IDH1* (14% versus 4%) was more frequently mutated in those with low *LILRB1* expression. High *LILRB5* expression was positively

correlated with *TP53* mutations and negatively correlated with *FLT3* and *WT1* mutations (Figure S13A). In addition, *RUNX1*-mutated AML highly expressed the *LILRB1* gene, and *TP53* mutations were linked to higher *LILRB5* expression (Figure 4B). For the other three genes, *LILRB2* was associated with mutations in *IDH1* and *STAG2*, *LILRB3* with *WT1*, and *LILRB4* with *RUNX1* (Figure 4B).

We also considered the possibility that specific regions of the genome may be preferentially focally amplified or deleted in patients with high or low *LILRB* expression. We therefore performed GISTIC2.0 analysis of TCGA copy-number data and assessed copy-number variations (CNVs) in two patient groups. We focused on *LILRB1*, as it was consistently dysregulated and showed the greatest mutational events in patients with AML. Interestingly, *LILRB1*^{low} patients had no somatic copy-number alterations (Figure S13B), whereas *LILRB1*^{high} patients had 14 significantly deleted regions and four significantly amplified regions (false discovery rate [FDR] = 0.25) (Figure 4D). Interestingly, the majority of genes deleted in *LILRB1*^{high} patients were involved in inflammatory responses (including cytokines and genes essential for microbial killing and antigen processing and presentation; see Table S1 for details). Also, a number of genes belong to the cadherin (*CDH*), protocadherin (*PCDH*) family (e.g., *CDH1*, *PCDH1*, and *PCDH12*), and cyclin-dependent kinase (*CDK*) inhibitors (e.g., *CDKN1B*, *CDKN2A*, and *CDKN2B*), which often exert tumor-suppressive functions,[25,26] were significantly deleted. In contrast, *LILRB*-high patients with AML had recurrent amplification at loci essential in AML pathogenesis, including *KMT2A* and *ERG* (Figure 4E).[27,28]

LILRB4 is aberrantly overexpressed in MLL-rearranged AML and may be a target of MLL fusion proteins

We next asked whether *LILRB* expression could be associated with specific molecular subtypes in AML. To this end, we examined the expression differences of *LILRB*s across published transcriptomic subtypes in the Hemap dataset (including AML, pre-B-ALL, diffuse large B cell lymphoma [DLBCL], and MM).[29] As expected, all five *LILRB* members were more highly expressed in monocyte-like AML, while their expressions were relatively weak in the other three malignancies (Figure 5A). One exception to this overall trend was the strong enrichment of *LILRB4* in MLL-rearranged AML (monocyte-like MLL) and ALL (KMT2A) (Figure 5A). This agreed favorably with previous findings that *LILRB4* was correlated with MLL-rearranged leukemia.[30,31] To further confirm this observation, we subsequently analyzed the transcript levels of *LILRB4* in 15 leukemia cell lines with or without MLL rearrangements from the CCLE database. Leukemia cell lines with the presence of MLL fusion genes exhibited markedly higher *LILRB4* expression than those lack MLL fusion genes, whether *LILRB4* expression was detected by RNA-seq (Figure 4B) or Affymetrix microarray (Figure S14A). Accordingly, analysis of three large primary patient datasets (BeatAML, TCGA, and GSE13159) revealed consistently higher *LILRB4* expression in MLL-rearranged AML compared with other cytogenetic/clinicopathologic leukemia entities (Figures 5C, S14B, and S14C). To further confirm the relevance of *LILRB4* expression in MLL-rearranged AML, we collected four MLL-rearrangement-related gene signatures from MSigDB and computed ssGSEA scores of these signatures for each sample in the TCGA dataset. Then, we compared the ssGSEA scores computed for high *LILRB4*-expressing samples with those in low *LILRB4*-expressing samples. We found gene sets down-regulated in MLL-rearranged AML (MULLIGHAN_MLL_SIGNATURE_1_DN) showed significantly lower ssGSEA scores in *LILRB4*-high patients than in *LILRB4*-low patients, whereas for gene sets up-regulated in MLL-rearranged AML (MULLIGHAN_MLL_SIGNATURE_1_UP), the opposite was seen (Figure 5D). Also, the ssGSEA scores of two MLL-rearranged-governed signatures (ROSS_AML_WITH_MLL_FUSIONS and VALK_AML_WITH_11Q23_REARRANGED) were significantly up-regulated in high *LILRB4* expressers (Figure S14D).

It has been shown that target genes of MLL fusions were often hypomethylated.[32,33] Consistently, significantly hypomethylated promoters of *LILRB*s were observed in both the Diseasemeth (AML, n = 271; normal, n = 10) and GSE63409 dataset (AML, n = 44; normal, n = 30) (Figures S15A and S15B). Moreover, the expression of *LILRB2*, *LILRB3*, and *LILRB4* correlated negatively with promoter methylation, and the most significant correlation was observed for *LILRB4* (Figure S15C). This observation is consistent with a previous report that decitabine (DAC; a demethylating agent) treatment with AML cells remarkably promoted the expression of *LILRB* family members, especially *LILRB4*.[34] Also, promoters of MLL fusion target genes were often enriched with transcription activation-associated histone markers (H3K79me2, H3K27ac, and H3K4me3).[35] To determine whether *LILRB4* expression could be directly regulated by the MLL fusion gene, we analyzed a published chromatin immunoprecipitation (ChIP)-seq dataset (GEO: GSE79899) of MLL fusion proteins H3K79me2, H3K27ac, and H3K4me3 for MV4-11 (MLL-AF4) and THP-1 (MLL-AF9) cell lines. We found a significant enrichment of MLL-N proteins in the promoter regions of *LILRB4* gene for both cell lines, while punctuated binding peaks of H3K79me2, H3K27ac, and H3K4me3 were observed in both the promoter and gene body of *LILRB4* (Figure 5E). Importantly, a similar enrichment of the three epigenetic marks was seen in five other ChIP-seq datasets (H3K79me2 from GEO: GSE82116 and GSE71779; H3K27ac from GEO: GSE89336 and GSE71776; H3K4me3 from GEO: GSE61785 and GSE82116) (Figure 5F). Overall, these results suggest that MLL fusion proteins may be a direct regulator of *LILRB4* expression.

Correlations between *LILRB*s and tumor immune infiltrating cells (TIICs) in AML

Considering that *LILRB*s might play important roles in the TME, we further explored the correlations between *LILRB*s and the level of immune cell infiltration in the TCGA AML cohort. It is noteworthy that, among the 22 cell types, monocytes had the highest positive correlations with *LILRB1*–*LILRB4*, while only a weak correlation was observed between *LILRB5* and monocytes (Figure 6A), consistent with the previous findings that *LILRB*s were preferentially expressed in monocytic AML.[19,31] This monocytic preference was also confirmed in two recently published single-cell RNA-seq (scRNA-seq) datasets of

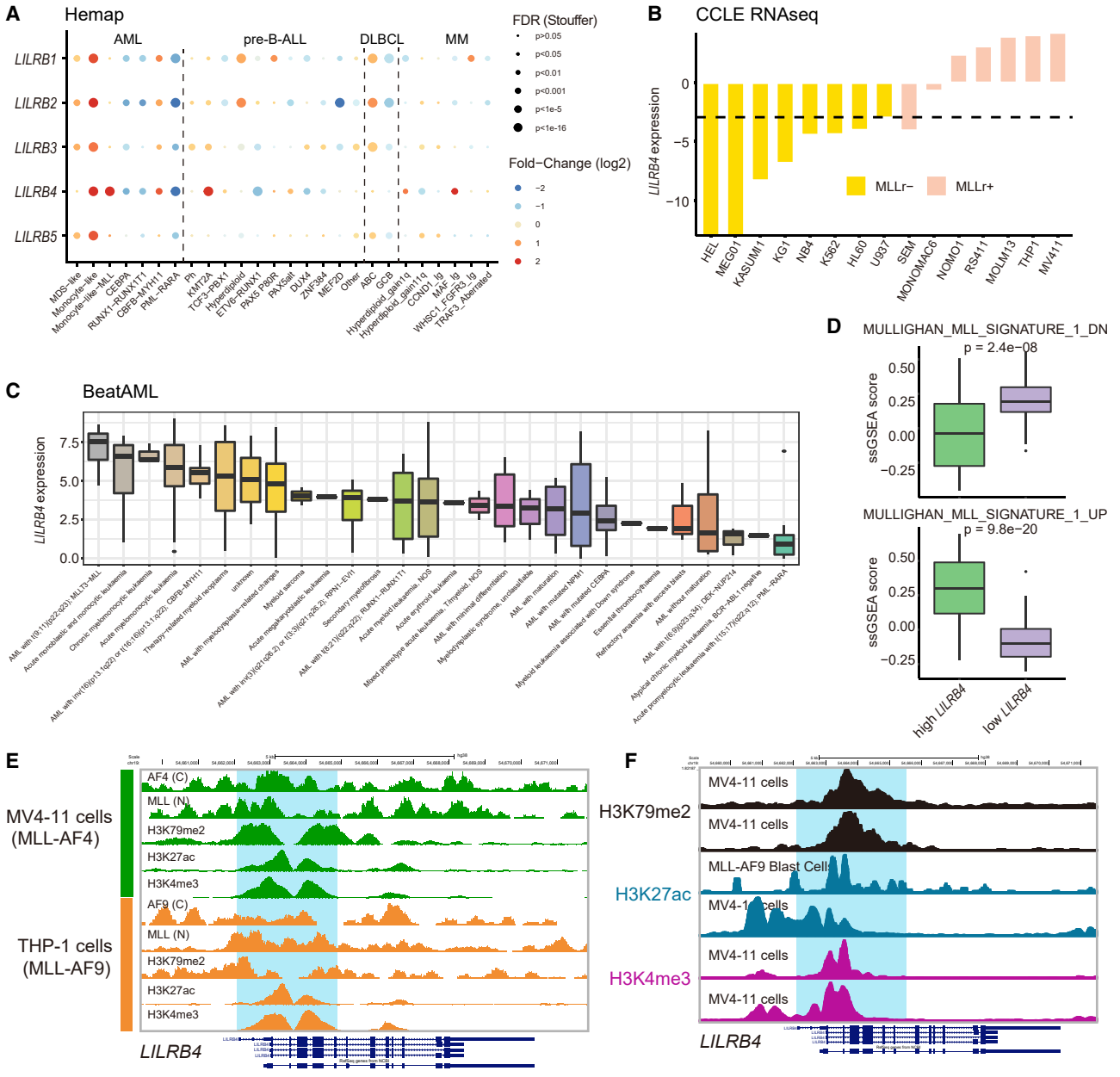

Figure 5. *LILRB4* is aberrantly overexpressed in MLL-rearranged AML and is likely a direct target of MLL fusion proteins

(A) Expression differences of *LILRB* genes in molecular subtypes of AML and pre-B-ALL, DLBCL, and MM. The expression FC between each subtype and the remaining samples in the same disease were compared using the Wilcoxon rank-sum test. The color of the dots indicates FCs (log2), and size indicates the FDR values. The FDR values were categorized into six groups based on significance cutoffs for visualization (0.05, 0.01, 0.001, 1×10^{-5}, 1×10^{-16}). (B) Bar plot showing *LIRB4* expression (RNA-seq) in non-MLL-rearranged (HEL, MEG01, KASUMI1, KG1, NB4, K562, HL60, U937) and MLL-rearranged (SEM, MONOMAC6, NOMO1, RS411, MOLM13, THP1, MV411) cell lines from the CCLE database. The dotted line represents the mean expression of *LILRB4* across all cell lines analyzed. (C) Comparison of *LILRB4* expression among human primary AML cases with MLL rearrangements and those without MLL rearrangements in the BeatAML dataset. (D) Box plots showing ssGSEA scores of two MLL-related gene signatures (MULLIGHAN_MLL_SIGNATURE_1_DN and MULLIGHAN_MLL_SIGNATURE_1_UP) between patients (TCGA dataset) with high and low *LILRB4* expression (as stratified by the median expression value). (E) ChIP-seq tracks for MLL fusion proteins, H3K79me2, H3K27ac, and H3K4me3 at *LILRB4* gene loci in MV4-11 and THP-1 cell lines. ChIP-seq data were obtained from GEO: GSE79899. (F) ChIP-seq tracks for H3K79me2, H3K27ac, and H3K4me3 at *LILRB4* gene loci in MV4-11- and MLL-AF9-transformed blast cells. ChIP-seq data were obtained from GEO: GSE82116, GSE71779, GSE89336, GSE71776, and GSE61785. See also Figures S14 and S15.

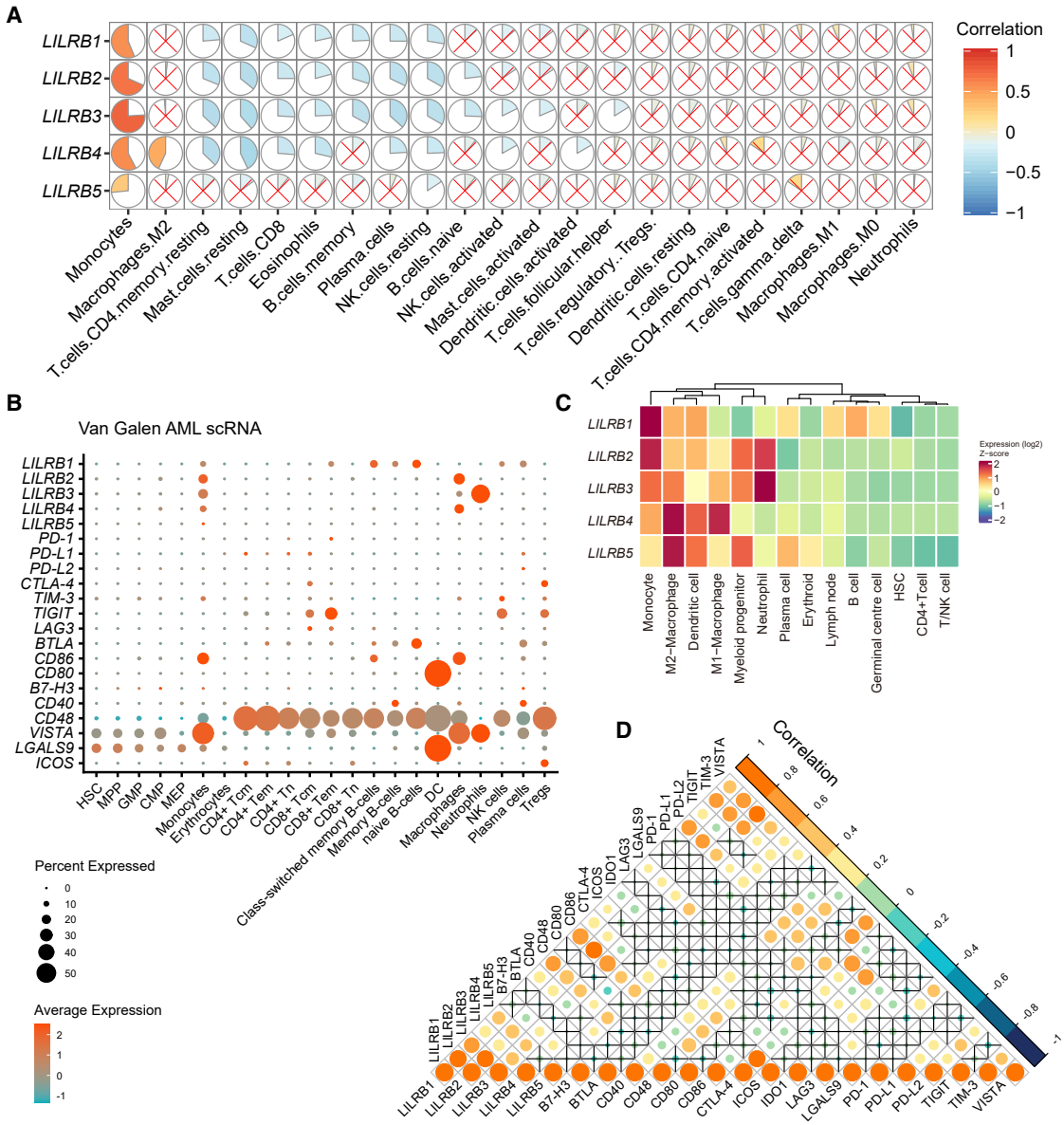

Figure 6. The relation between *LILRBs* expression with immune cell infiltration and immune checkpoints

(A) Correlation matrix plot showing correlations between *LILRBs* and tumor immune infiltrating cells (TIICs). The overall immune cell compositions were estimated by CIBERSORT in the TCGA dataset. (B) Dot plot showing expression pattens of *LILRBs* and selected immune checkpoint genes in annotated cell types from 16 AML scRNA-seq samples (Van Galen AML scRNA). The color of the dots indicates average expression, and size indicates percentage of cells with detectable expression. (C) Heatmap showing *LILRB* expression in normal cell populations from the Hemap dataset. (D) Correlogram showing correlations between the expression of *LILRBs* and selected immune checkpoint genes in the TCGA dataset. Positive correlation was marked with orange and negative correlation with blue. See also Figure S16.

AML (Van Galen AML scRNA, Figure 6B, and FIMM AML scRNA, Figure S16A). Interestingly, *LILRB4* was exclusively correlated with M2 macrophages (Figure 6A), a high immunosuppressive component in the TME. By contrast, *LILRB1–LIRB4* were negatively correlated with the infiltrating levels of tumor-suppressive immune cells, such as resting memory CD4 T cells, CD8 T cells, memory B cells, plasma cells, and resting natural killer (NK) cells (Figure 6A). Similar results were found by analyzing the CIBERSORT estimates in the GEO: GSE10358 and GSE6891 datasets (Figures S16B and S16C). Importantly, when other methods were used for calculating the relative fractions of TIICs, positive associations between *LIRB1–LILRB4* and monocytes were consistently seen, while negative associations between *LILRB1–LILRB4* and CD8 T cells were proved for most, if not all, methods in all three datasets (Figures S16D–S16F). Further analysis of normal cell populations from the Hemap dataset revealed that *LILRBs* were highly expressed in myeloid lineage immune cells

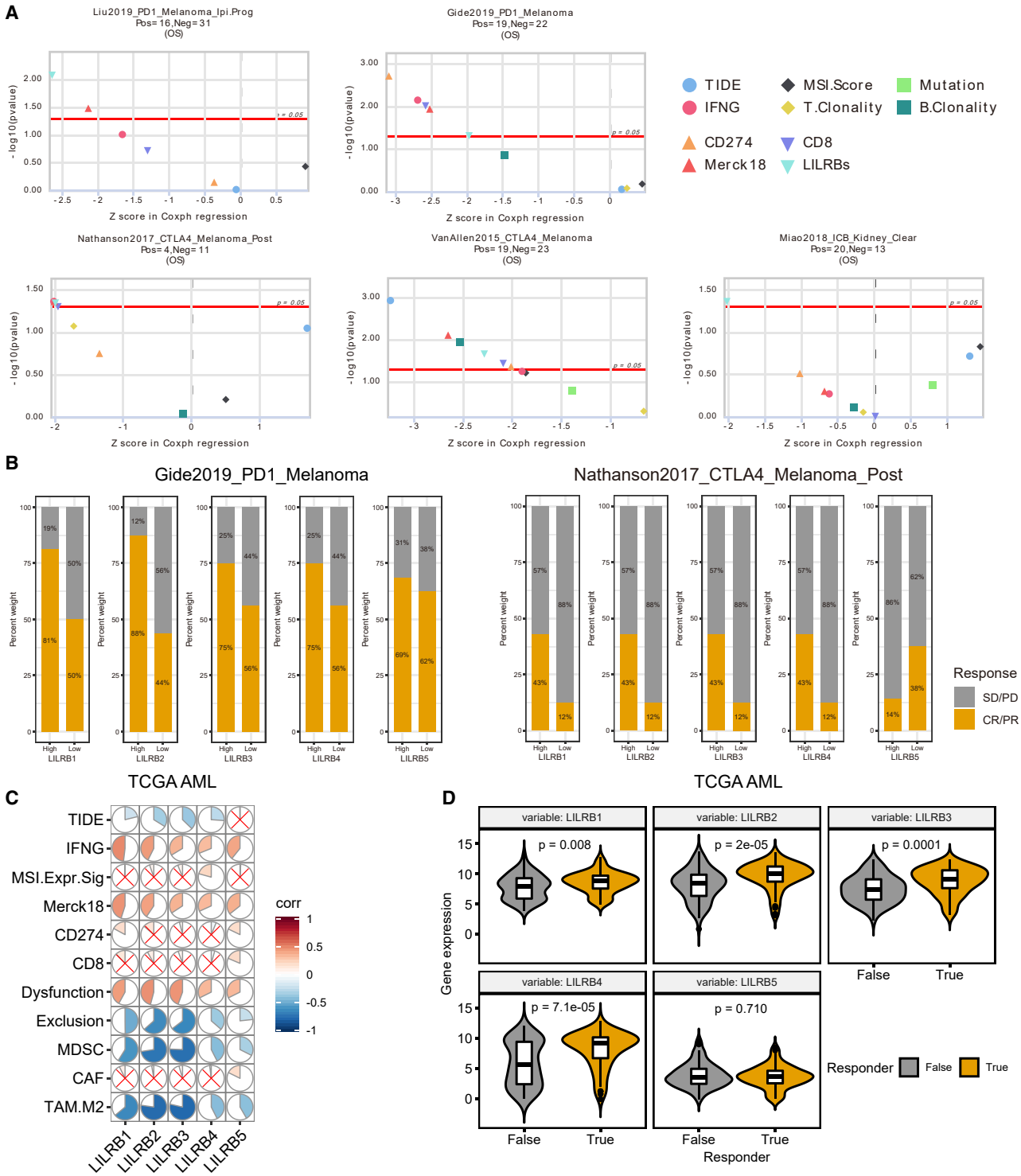

Figure 7. *LILRB* expression predicts responses to immunotherapy

(A) Scatterplot comparing predict performance of *LILRB*s to that of standardized cancer immune evasion biomarkers for OS among indicated ICB cohorts. The x axis denotes the *Z* score on Cox-PH regression, and the y axis indicates its significance level (two-sided Wald test). The red horizontal line in each plot indicates threshold for significance (p = 0.05). (B) Percentages of responders (complete response [CR] or partial response [PR]) and non-responders (stable disease [SD] or progressive disease [PD]) to ICB

(legend continued on next page)

(monocytes, macrophages, dendric cells, myeloid progenitors, and neutrophils), with consistent low expression in T cells (CD4+ T cells and T/NK cells) (Figure 6C). Collectively, these findings further confirmed the immunosuppressive roles of *LILRB*s in cancer TME.

Correlation between *LILRB*s and immune checkpoints in AML

Given that immune checkpoints have been proven to be promising therapeutic targets for cancer treatment, we therefore evaluated the relationship between *LILRB*s and a collection of checkpoint genes describe by De Simone et al.[36] Results from Spearman correlation analyses are given in Table S2. As shown in the correlogram, *LILRB1*–*LILRB3* all showed strong positive correlations with *CD48*, *CD86*, *PD-L2*, *TIM-3*, and *VISTA* (Figure 6D), while relatively weaker associations were observed between *LILRB4*/5 and these checkpoints. Moreover, analysis at the single-cell level revealed that *CD86* and *VISTA*, which, like *LILRB*s, were preferentially expressed in monocytes (Figures 6B and S16A). In contrast, *LILRB*s did not show any correlations with *PD-1*, and only weak correlations between *CTLA-4* and *LILRB*s (except for *LILRB4*) were observed (Figure 6D). These results further highlight *LILRB*s potentially as major signaling pathways involved in immunosuppression in the AML microenvironment.

LILRB expression predicts responses to immunotherapy

Considering the strong connection between *LILRB* expression and immune response, we next asked whether *LILRB* expression can be utilized as a tool to predict response to immune checkpoint blockade (ICB). We first used Tumor Immune Dysfunction and Exclusion (TIDE; http://tide.dfci.harvard.edu/) to assess the potential of *LILRB*s as new biomarkers by comparing their predictive power with that of existing biomarkers. Surprisingly, we found that *LILRB*s had an area under the curve (AUC) of >0.5 in 17 of the 22 (77%) ICB subcohorts, comparable to the predictive performance of TIDE (18 out of 25, 72%). It also showed a higher predictive value than tumor mutational burden (TMB), T clonality, and B clonality (Figure S17). Moreover, our analyses revealed that *LILRB*s could predict patients' survival in five independent immunotherapy cohorts, including two melanoma cohorts treated with anti-PD-1 therapy (Liu2019_PD1_Melanoma and Gide2019_PD1_Melanoma), two melanoma cohorts treated with anti-CTLA-4 therapy (Nathanson2017_CTLA4_Melanoma_Post and VanAllen2015_CTLA4_Melanoma), and one clear cell renal cell carcinoma (ccRCC) cohort with anti-PD-1 monotherapy (Miao2018_ICB_Kidney_Clear). Remarkably, *LILRB*s exhibited the highest predictive value in three of the five datasets (Figure 7A). In the Gide2019_PD1_Melanoma and Nathanson2017_CTLA4_Melanoma_Post cohorts, the percentage of responders (complete response [CR] or partial response [PR]) to ICB was generally higher in patients with high *LILRB* expression than those with low *LILRB* expression (Figure 7B). Similar findings could be extended to other cancer types (lung cancer and gastric cancer) with ICB treatment (Jung2019_PD1/PDL1_ Lung and Kim2018_PD1_Gastric) and melanoma patients treated with adoptive T cell therapy (ACT) (Lauss2017_ACT_Melanoma) (Figure S18). In addition, high *LILRB* expressions were generally correlated with *PD-1*/*CTLA-4* up-regulation in cohorts treated with respective antibodies (Figure S19A). To test the potential of *LILRB*s in predicting ICB response in patients with AML, we checked the relationship of *LILRB*s with expression signatures for predicting ICB response in the TCGA AML dataset. Surprisingly, we found a negative correlation of *LILRB*s with T cell-exclusion signatures, including myeloid-derived suppressor cells (MDSCs), M2 subtype of tumor-associated macrophages (TAMs), exclusion, and TIDE (except for *LILRB5*) score but a positive correlation with the T cell dysfunction score, interferon gamma (IFNG), and merck18 signatures (Figure 7C). These observations indicate that *LILRB*s might contribute to immune evasion through the induction of T cell dysfunction. In the TCGA AML cohort, we found that *LILRB*s (except for *LILRB5*) showed significantly higher expression in predicted responders than non-responders (Figure 7D), suggesting that AML with high *LILRB* expression may benefit more from ICB treatment. While no differences in *PD-1* expression between low and high *LILRB*s expressers were observed, patients with high *LILRB*s showed an obviously high expression of *CTLA-4* in the TCGA AML cohort (Figure S19B).

The biological significance of *LILRB* expression in AML

We then sought to investigate the biological features associated with *LILRB*s in AML. Since the expressions of five *LILRB* members were highly correlated, a comparison of gene expression profiles of patients with high and low *LILRB1* expression (as determined by the median expression value) was performed. Overall, 799 genes (490 up- and 309 down-regulated; adjusted $p < 0.05$; log2 fold change [FC] $\leq$ -1.5 or $\geq$ 1.5) were differentially expressed in $LILRB1^{high}$ versus $LILRB1^{low}$ patients (Figure 8A; Table S3). Among the genes positively correlated with *LILRB1* were, as expected, the other members of the *LILRB* family (Figure 8A). Also, genes associated with the presence of monocytes/macrophages (*CD14*, *CD68*) or M2 macrophage polarization (*MSR1*, *MRC1*, *CD163*) were significantly up-regulated in high *LILRB1* expressers (Figure 8A), in line with our previous findings. Next, we used the STRING database to construct a protein-protein interaction (PPI) network of the differentially expressed genes (DEGs), with a confidence score >0.90. Genes interacting with *LILRB1* and their subnetworks were shown through Cytoscape software (Figure 8B). We found 12 genes directly interacting with *LILRB1*: *PILRA*, *TLR8*, *SIGLEC7*, *CD300C*, *FCGR2A*, *FCGR2B*, *FCGR3A*, *CD86*, *FGR*, *HCK*, *IL10*, and *ITGAX*. Among them, *CD300C*, *FCGR2A*, *FCGR2B*, and *FCGR3A* also had connections with the other four *LILRB* members (Figure 8B). GeneMANIA results also revealed that genes of the *FCGR* and *CD300* family were closely correlated with *LILRB*s. These genes were mainly involved in negative regulation of leukocyte-mediated immunity and negative regulation of the immune-system process (Figure S20A).

among indicated ICB cohorts between patients with high and low *LILRB* expression (as stratified by the median expression value of respective genes). (C) Correlogram showing the association between *LILRB* expression with T cell-dysfunction and T cell-exclusion signatures in TCGA AML cohort, as determined using the tumor immune dysfunction and evasion (TIDE) method. (D) Violin plots comparing the expression of *LILRB*s between patients who benefitted and did not benefit from immunotherapy in AML, as predicted by the TIDE algorithm. Significances were calculated by Wilcoxon rank-sum tests. See also Figures S17–S19.

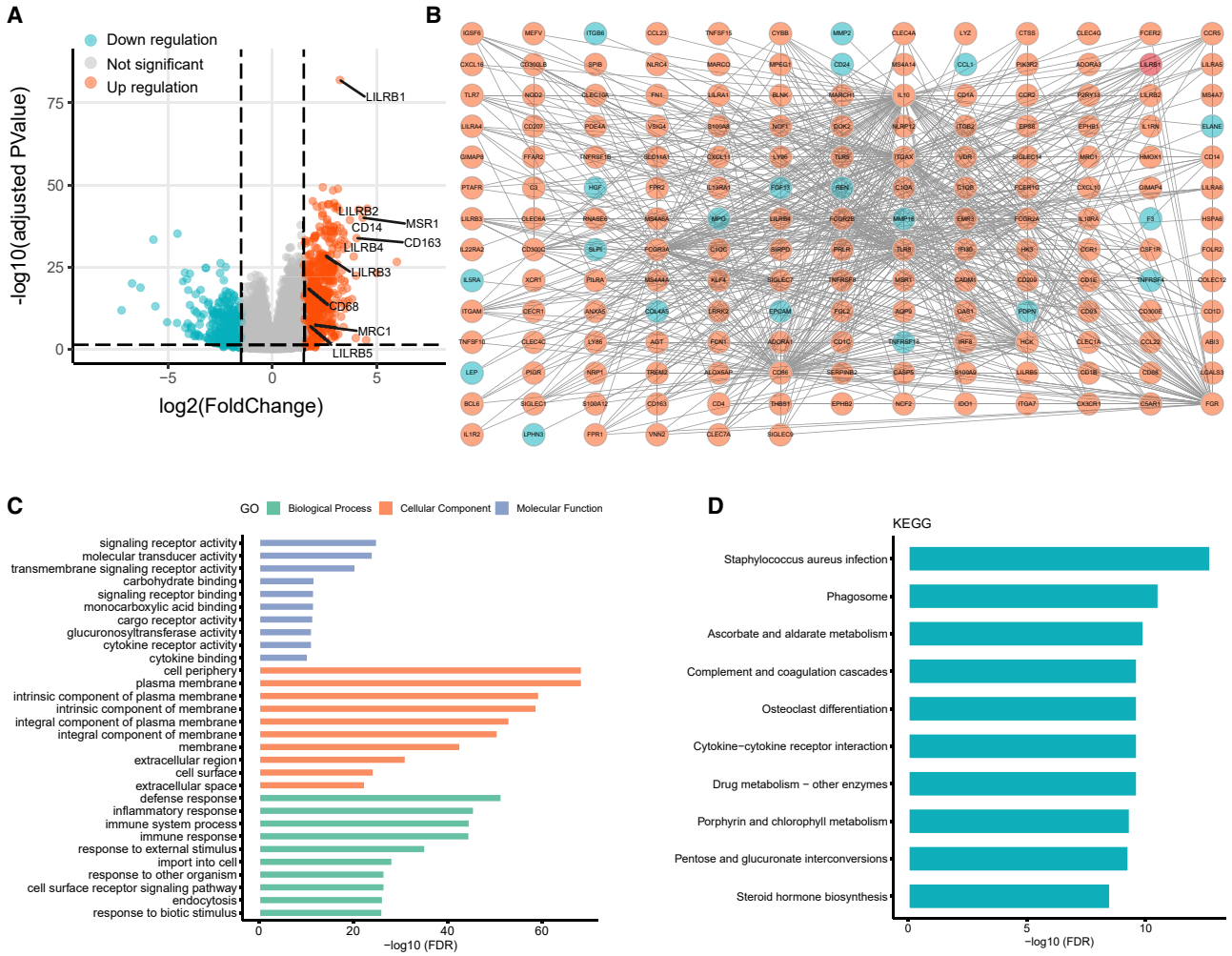

Figure 8. The biological significance of *LILRBs* expression in AML

(A) Volcano plot showing differentially expressed genes (DEGs) between high and low *LILRB1* expressers (as stratified by the median expression value). (B) Cytoscape analysis of *LILRB1*-related network using PPI information obtained from STRING database (http://stringdb.org/). Red nodes represent up-regulated genes and blue represent down-regulated genes. (C and D) GO (C) and KEGG (D) analysis of DEGs. See also Figures S20 and S21.

We then performed Gene Ontology (GO) analysis using these DEGs, and the top 10 significant terms of biological process (BP), molecular function (MF), and cellular component (CC) enrichment analysis were shown (Figure 8C). Notably, in terms of BP, immune-response-related processes were significantly enriched, such as inflammatory response, immune-system process, and immune response. Kyoto Encyclopedia of Genes and Genomes (KEGG) and Reactome Pathway analyses also revealed immune-response pathways, including cytokine-cytokine receptor interaction, cytokine signaling in immune system, innate immune system, antigen processing-cross presentation, and adaptive immune system, were mainly enriched (Figures 8D and S20B).

Finally, gene set enrichment analysis (GSEA) was conducted in the *LILRB1*^{high} and *LILRB1*^{low} cohorts. For the C2 collection of curated gene sets from the MSigDB, the VALK_AML_CLUSTER_5 gene set (96% of the samples are FAB M4 or M5 subtype) was predominantly enriched in the *LILRB1*^{high} group. Also enriched were gene sets of MLL fusion and *NPM1* mutation, two distinct entities often associated with monocytic features of AML (Figure S21A). For the C7 immunologic collection, the *LILRB1*^{high} group had principal enrichment in genes up-regulated in monocytes compared with other immune cells (Figure S21B), and multiple immune activities were enriched in the *LILRB1*^{high} group for HALLMARK gene sets (Figure S21C).

DISCUSSION

The *LILRB* family members *LILRB1–LILRB5* are a group of proteins containing the immune-inhibitory ITIM motifs that negatively regulate immune cell activation.[14] Here, using RNA-seq data of normal

tissues from GTEx, FANTOM5, and HPA, we showed that *LILRB* members were predominantly enriched in the spleen, consistent with their immune-modulatory functions. In cancer cell lines, *LILRBs* showed relatively high expression in cell lines of malignant hematological origin, in line with the selective expression of *LILRBs* in hematopoietic lineage cells. Indeed, abnormal expression of *LILRBs* has been documented in various cancers, such as lung cancer,[37] hepatocellular carcinoma (HCC),[38] and certain types of subtypes of adenocarcinoma.[39] In this study, based on combined datasets from TCGA and GTEx, we comprehensively analyzed *LILRB* expression between tumor and adjacent normal tissue across 28 cancer types (9,465 tumor and 7,831 normal samples). Our data showed that *LILRBs* were significantly dysregulated in the majority of tumor types. For *LILRB1–LILRB4*, the most striking difference was seen between AML and its normal counterparts. We also observe a strong enrichment for *LILRB1–LILRB4* in the monocytic lineage; this observation was confirmed in mass spectrometry proteomic data, single-cell transcriptomics of immune cells, immune cell abundances estimated using bulk TCGA samples, and GSEA of monocyte-related gene sets, in agreement with previous reports.[19,21,31,40] One limitation is that many of the findings were based on correlation analyses; the results could, therefore, be biased by normalization methods and statistical analyses along the way. Future functional immunological data and prospective validation will still be required before these *in silico* approaches can be used in a clinical setting.

Despite being positively correlated with monocytes, *LILRB1–LILRB4* were negatively correlated with the density of CD8+ T and NK cells, which are considered essential for effective anti-tumor immunity.[29] It has been shown that activated *LILRB4* on monocytic AML cells recruits *SHP-2* and upregulates nuclear factor κB (*NF-κB*), leading to increased *ARG1* and *uPAR* accompanied by a concomitant suppression of T cell activity.[18,19] This might provide a potential mechanistic explanation to our observations. It should be noted that BM T cells in AML are often functionally impaired,[11–13,41] possibly mediated by malignant monocyte-like cells from AML.[11,19,20,42] Further research aimed at unraveling the underlying molecular mechanisms is clearly warranted, as this may provide opportunities for the identification of new drug targets and therapeutics that can circumvent the T cell-suppression state in AML.

Immunosuppressive factors, such as indoleamine 2,3-dioxygenase 1 (*IDO1*), *CD200*, and *TIM-3* were reported to be closely associated with a poor outcome in AML.[43–45] In a preliminary analysis, Deng et al. studied the prognostic relevance of several co-stimulating and co-inhibitory receptors in the TCGA AML dataset, including *LILRB1–LILRB4*.[19] Here, we independently validated the prognostic significances of *LILRB* members in five independent datasets. Strikingly, we showed that *LILRB1–LILRB4* adversely impacted survival in almost all analyzed datasets. Of interest, we also noticed that *LILRB4* was significantly associated with M2 macrophage abundances. This observation raises the possibility that *LILRB4* might contribute to leukemogenesis through M2 macrophages. Our group has recently reported that M2 macrophage fractions were more selectively up-regulated in AML than the other four hematological malignancies and normal controls.[10] Importantly, we also demonstrated superior predictive performance of the M2 marker *CD206* (*MRC1*) than classical prognosticators in AML. Interestingly, in this study, we found that *CD206* was significantly up-regulated in high *LILRB1* expressers. As *CD206*+ and/or *LILRB4*+ monocytes could suppress T cell proliferation and create an immunosuppressive microenvironment in AML,[19,42] it could be hypothesized that at least part of the prognostic value of *LILRBs* could be attributed to the immune-suppressive TME it contributed. Acute monocytic leukemia often harbors mixed-lineage leukemia (MLL) rearrangements, an aggressive phenotype with limited treatment options and poor survival rates, which might also explain the observed result. Indeed, we demonstrated that *LILRB4* was aberrantly overexpressed in MLL-rearranged AML and might be a direct target of the MLL fusion proteins.

In a recent pan-hematological-malignancies study, the authors found that *LILRB2* could distinguish lymphoma and leukemia subtypes with high immune infiltration from those harboring lower cytolytic score.[29] We consistently found multiple genes involved in immune activation (including cytokines and genes essential for microbial killing and antigen processing and presentation) were deleted in *LILRB1*^{high} patients, indicating a delicate balance between immune activation and suppression in the TME.

Indeed, an integrated analysis of transcriptomic and proteomic data has uncovered and ranked *LILRBs* among the top potential chimeric antigen receptor (CAR) targets in AML.[46] Gui et al. also found that blocking *LILRB4* activation effectively reversed T cell suppression and inhibited AML cell infiltration.[18] Given that *LILRBs* are selectively dysregulated in AML, it is tempting to speculate that AML positive for these proteins might be good candidates for immunotherapy. Indeed, we found that *LILRBs* showed comparable or even superior predictive power for ICB response than other biomarkers reported in the literature, as quantified both by AUC and *Z* score in the Cox proportional hazard (PH) regression. This agreed favorably with our observation that patients with high *LILRB* expression possessed primarily immune-enriched subtypes, which were characterized by highly abundant lymphocytes, increased *PD-L1* expression, and amplifications of *PD-L1* and *PD-L2* genes,[24] suggesting an environment with dampened anti-tumor immunity that could benefit from immunotherapy. Also, we found high *LILRB* expressers often exhibited increased *PD-1*/*CTLA-4* expression in ICB cohorts. Our findings were in line with previous observations that *LILRB2* was co-expressed with *CTLA-4* and that patients responding to anti-*PD-1* ICB showed an enriched expression of *LILRB4*.[47,48] Importantly, Chen et al. reported that *LILRB2* blockade substantially enhanced the efficacy of anti-*PD-1* treatment in a human lung cancer model.[49] We also demonstrated the predictive potential of *LILRBs* in AML immunotherapy. Although we observed no correlations between *LILRBs* and *PD-1* expression in AML, *LILRB* agonism could reprogram TAMs into a non-suppressive and immunostimulatory phenotype, thereby enhancing the

therapeutic efficacy of ICB treatment.[49] Future cancer immunotherapy clinical trials will be critical to further validate these findings.

In this study, we provided a comprehensive analysis of the expression patterns and clinical significances of *LILRB*s across pan-cancers, focusing on their role in AML. We also analyzed the association of *LILRB* expression with genomic features and tumor immunity in AML. Our data revealed up-regulated expression of *LILRB*s in AML and that higher expression levels of these genes predicted worse outcomes. In addition, *LILRB*s were associated with an immune-suppressive TME in AML. Overall, these findings suggest important immunological and clinical implications of *LILRB*s in AML, which warrants further clinical investigation with immunotherapy specifically targeting AML with *LILRB* dysregulations.

MATERIALS AND METHODS

Analysis of gene-expression data

Briefly, the mRNA expression data of the *LILRB* family in normal tissues were obtained from the GTEx project (www.gtexportal.org/).[50] Datasets used to assess the expression patterns of *LILRB*s in normal tissues and cell lines are described in detail in the supplemental methods. To determine the expression patterns of *LILRB*s between tumor and adjacent normal tissues across a broad range of cancer types, we systematically analyzed the gene-expression data of 9,465 tumor and 7,831 normal samples based on RNA-seq data from the TCGA and GTEx projects. All these datasets were downloaded from the UCSC Xena project and were normalized between arrays using the limma package.[51] These studies were approved by the respective institutional review boards with written informed consent obtained from all patients.

Analysis of AML scRNA-seq data

For scRNA data analysis, previously published scRNA-seq data from 16 AML samples at diagnosis consisting of 30,712 BM cells (Van Galen AML scRNA) were downloaded from GEO (GEO: GSE116256).[11] Another scRNA-seq data for 8 patients consisting of 30,579 AML BM cells (FIMM AML scRNA) were retrieved via the Synapse Web Portal (https://www.synapse.org and https://doi.org/10.7303/syn21991014). Data were processed and visualized using custom scripts provided by Dufva et al.[29]

Analysis of genetic alteration data

The genetic alterations of *LILRBs* from TCGA PanCancer Atlas studies (10,967 patients), including somatic mutations, amplification, and deep deletion, were assessed through the cbioportal for Cancer Genomics (http://www.cbioportal.org). Procedure details are provided in the supplemental methods.

Analysis of gene-methylation data

For comparison of methylation status of *LILRB*s between tumor and normal samples, beta values of Illumina 450k probes at the promoter region of five genes were retrieved by the DiseaseMeth v.2.0 web portal (http://bio-bigdata.hrbmu.edu.cn/diseasemeth/analyze.html). Procedure details are provided in the supplemental methods.

Analysis of the association between *LILRB4* and MLL rearrangement

We used the Hemap dataset to analyze the association between *LILRB* expression and common molecular subtypes.[29] Datasets used to determine the association of *LILRB4* expression with MLL rearrangement and analysis of ChIP-seq data are described in detail in the supplemental methods.

Survival analysis

We investigate the association between the expression of *LILRB* members and clinical outcomes across 33 cancer types. The association between transcript levels of *LILRB* members and OS across cancers were assessed by univariate Cox regression. To confirm the prognostic value of *LILRB*s in AML, we further obtained five independent GEO datasets (GEO: GSE10358, n = 304; GSE37642 [U133A], n = 422; GSE37642 [U133plus2], n = 140; GSE106291, n = 250; GSE71014, n = 104) with available survival information. Patients with AML from these datasets and the TCGA dataset were divided into those with high and low gene expression, according to the optimal cutoff determined by the X-tile method.[52] We then performed Kaplan-Meier analysis (log rank test) to compare the survival differences of two groups regarding OS (six datasets) and EFS (only in TCGA dataset).

Immune-response analysis

The relative abundances of 22 immune cell populations in patients with AML were estimated using the CIBERSORT algorithm, as previously described.10 As CIBERSORT may not be suitable for the use of the RNA-seq data,[53] this algorithm was exclusively applied to the TCGA LAML microarray dataset. For validation purposes, the relative fractions of immune cells were also estimated in two relatively large GEO datasets, GEO: GSE10358 and GSE6891. In addition, we used other deconvolution methods to quantify the proportions of monocytes (quanTIseq, MCP-counter, CIBERSORT abs, and xCell) and CD8 T cells (EPIC, TIMER, quanTIseq, MCP-counter, CIBERSORT abs, and xCell). These methods have been integrated as a unified interface by Sturm et al. and are freely available through the TIMER 2.0 web portal (http://timer.comp-genomics.org/).[54] We evaluated the relationship between *LILRB*s and several notable immune checkpoint genes.36 Spearman correlation analysis was used to test the association between *LILRB* expression and these parameter estimates. Immunotherapy-associated dataset collection and analyses are provided in the supplemental methods.

Differential gene-expression analysis and functional enrichment analysis

Differential gene-expression analysis for RNA-seq data was performed using the raw read counts with the R/Bioconductor package "DESeq2," controlled for the FDR by the Benjamini–Hochberg procedure. GO analysis and KEGG pathway analysis of *LILRB1*-co-expressed genes were performed using the STRING database (http://www.string-db.org/). GO and KEGG terms with FDR-corrected p values less than

0.05 were considered significantly enriched. For displaying purposes, the top 10 GO terms of each three GO categories—BP, CC, and MF—and the top 10 KEGG pathway terms were visualized as bar plots.

PPI-network analysis

We applied STRING (http://string.embl.de/) to construct a PPI network of the DEGs. We chose a confidence score >0.9 as the judgment criterion. Cytoscape visualization software (v.3.6.1) was used to present the *LILRB1*-related subnetwork.

GSEA

GSEA was performed on the TCGA dataset using GSEA v.4.1.0 software (http://www.broad.mit.edu/gsea). Procedure details are provided in the supplemental methods.

Statistical analysis and visualization

All statistical analyses and visualizations were performed using either indicated web servers or R v.4.0.4. For details, see the supplemental methods.

Data and code availability

The datasets analyzed in this study are available in the following open access repositories: GTEx, www.gtexportal.org/; HPA, https://www.proteinatlas.org/; CCLE, https://www.broadinstitute.org/ccle; Human Proteome Map, https://www.humanproteomemap.org/; TCGA, https://portal.gdc.cancer.gov/; UCSC Xena, https://xena.ucsc.edu; cBioPortal, http://www.cbioportal.org; GEO, https://www.ncbi.nlm.nih.gov/geo/ (GEO: GSE13159, GSE116256, GSE63409, GSE79899, GSE82116, GSE71779, GSE89336, GSE71776, GSE61785, GSE10358, GSE37642, GSE106291, and GSE71014); FIMM AML scRNA data, https://www.synapse.org (https://doi.org/10.7303/syn21991014); DiseaseMeth, http://bio-bigdata.hrbmu.edu.cn/diseasemeth/analyze.html; TIMER 2.0, http://timer.comp-genomics.org/; and TIDE, http://tide.dfci.harvard.edu/.

SUPPLEMENTAL INFORMATION

Supplemental information can be found online at https://doi.org/10.1016/j.omto.2022.05.011.

ACKNOWLEDGMENTS

This study was supported by the National Natural Science Foundation of China (81970118, 81900163); the Medical Innovation Team of Jiangsu Province (CXTDB2017002); the Zhenjiang Clinical Research Center of Hematology (SS2018009); the Social Development Foundation of Zhenjiang (SH2019065 and SH2019067); and the Scientific Research Project of The Fifth 169 Project of Zhenjiang (21).

AUTHOR CONTRIBUTIONS

J.Q., J.L., and Z.-w.M. conceived and designed the study; Z.-j.X., X.-l.Z., Y.J., S.-s.W., and Y.G. collected and assembled data; Z.-j.X., J.-c.M., X.-m.W., and J.-y.L. performed data analysis; Z.-j.X. drafted the manuscript; J.Q., J.L., and Z.-w.M. participated in study supervision and commented on the manuscript. All authors read and approved the final manuscript.

DECLARATION OF INTERESTS

The authors declare that they have no competing interests.

REFERENCES

1. Löwenberg, B., Downing, J.R., and Burnett, A. (1999). Acute myeloid leukemia. N. Engl. J. Med. *341*, 1051–1062.
2. Byrd, J.C., Mrózek, K., Dodge, R.K., Carroll, A.J., Edwards, C.G., Arthur, D.C., Pettenati, M.J., Patil, S.R., Rao, K.W., Watson, M.S., et al. (2002). Pretreatment cytogenetic abnormalities are predictive of induction success, cumulative incidence of relapse, and overall survival in adult patients with de novo acute myeloid leukemia: results from Cancer and Leukemia Group B (CALGB 8461). Blood *100*, 4325–4336.
3. Marcucci, G., Mrózek, K., and Bloomfield, C.D. (2005). Molecular heterogeneity and prognostic biomarkers in adults with acute myeloid leukemia and normal cytogenetics. Curr. Opin. Hematol. *12*, 68–75.
4. Döhner, H., Estey, E.H., Amadori, S., Appelbaum, F.R., Büchner, T., Burnett, A.K., Dombret, H., Fenaux, P., Grimwade, D., Larson, R.A., et al. (2010). Diagnosis and management of acute myeloid leukemia in adults: recommendations from an international expert panel, on behalf of the European LeukemiaNet. Blood *115*, 453–474.
5. DiNardo, C.D., Pratz, K.W., Letai, A., Jonas, B.A., Wei, A.H., Thirman, M., Arellano, M., Frattini, M.G., Kantarjian, H., Popovic, R., et al. (2018). Safety and preliminary efficacy of venetoclax with decitabine or azacitidine in elderly patients with previously untreated acute myeloid leukaemia: a non-randomised, open-label, phase 1b study. Lancet Oncol. *19*, 216–228.
6. DiNardo, C.D., Maiti, A., Rausch, C.R., Pemmaraju, N., Naqvi, K., Daver, N.G., Kadia, T.M., Borthakur, G., Ohanian, M., Alvarado, Y., et al. (2020). 10-day decitabine with venetoclax for newly diagnosed intensive chemotherapy ineligible, and relapsed or refractory acute myeloid leukaemia: a single-centre, phase 2 trial. Lancet Haematol. *7*, e724–e736.
7. Perl, A.E. (2017). The role of targeted therapy in the management of patients with AML. Hematol. Am. Soc. Hematol. Educ. Program *2017*, 54–65.
8. Topalian, S.L., Hodi, F.S., Brahmer, J.R., Gettinger, S.N., Smith, D.C., McDermott, D.F., Powderly, J.D., Carvajal, R.D., Sosman, J.A., Atkins, M.B., et al. (2012). Safety, activity, and immune correlates of anti-PD-1 antibody in cancer. N. Engl. J. Med. *366*, 2443–2454.
9. Lichtenegger, F.S., Krupka, C., Haubner, S., Köhnke, T., and Subklewe, M. (2017). Recent developments in immunotherapy of acute myeloid leukemia. J. Hematol. Oncol. *10*, 142.
10. Xu, Z.J., Gu, Y., Wang, C.Z., Jin, Y., Wen, X.M., Ma, J.C., Tang, L.J., Mao, Z.W., Qian, J., and Lin, J. (2020). The M2 macrophage marker CD206: a novel prognostic indicator for acute myeloid leukemia. Oncoimmunology *9*, 1683347.
11. van Galen, P., Hovestadt, V., Wadsworth Ii, M.H., Hughes, T.K., Griffin, G.K., Battaglia, S., Verga, J.A., Stephansky, J., Pastika, T.J., Lombardi Story, J., et al. (2019). Single-cell RNA-seq reveals AML hierarchies relevant to disease progression and immunity. Cell *176*, 1265–1281.e4.
12. Lamble, A.J., Kosaka, Y., Laderas, T., Maffit, A., Kaempf, A., Brady, L.K., Wang, W., Long, N., Saultz, J.N., Mori, M., et al. (2020). Reversible suppression of T cell function in the bone marrow microenvironment of acute myeloid leukemia. Proc. Natl. Acad. Sci. USA *117*, 14331–14341.
13. Noviello, M., Manfredi, F., Ruggiero, E., Perini, T., Oliveira, G., Cortesi, F., De Simone, P., Toffalori, C., Gambacorta, V., Greco, R., et al. (2019). Bone marrow central memory and memory stem T-cell exhaustion in AML patients relapsing after HSCT. Nat. Commun. *10*, 1065.
14. Kang, X., Kim, J., Deng, M., John, S., Chen, H., Wu, G., Phan, H., and Zhang, C.C. (2016). Inhibitory leukocyte immunoglobulin-like receptors: immune checkpoint proteins and tumor sustaining factors. Cell Cycle *15*, 25–40.
15. Banchereau, J., Zurawski, S., Thompson-Snipes, L., Blanck, J.P., Clayton, S., Munk, A., Cao, Y., Wang, Z., Khandelwal, S., Hu, J., et al. (2012). Immunoglobulin-like transcript receptors on human dermal CD14+ dendritic cells act as a CD8-antagonist to control cytotoxic T cell priming. Proc. Natl. Acad. Sci. USA *109*, 18885–18890.
16. Baudhuin, J., Migraine, J., Faivre, V., Loumagne, L., Lukaszewicz, A.C., Payen, D., and Favier, B. (2013). Exocytosis acts as a modulator of the ILT4-mediated inhibition of neutrophil functions. Proc. Natl. Acad. Sci. USA *110*, 17957–17962.

17. van der Touw, W., Chen, H.M., Pan, P.Y., and Chen, S.H. (2017). LILRB receptor-mediated regulation of myeloid cell maturation and function. Cancer Immunol. Immunother. *66*, 1079–1087.

18. Gui, X., Deng, M., Song, H., Chen, Y., Xie, J., Li, Z., He, L., Huang, F., Xu, Y., Anami, Y., et al. (2019). Disrupting LILRB4/APOE interaction by an Efficacious humanized antibody reverses T-cell suppression and blocks AML development. Cancer Immunol. Res. *7*, 1244–1257.

19. Deng, M., Gui, X., Kim, J., Xie, L., Chen, W., Li, Z., He, L., Chen, Y., Chen, H., Luo, W., et al. (2018). LILRB4 signalling in leukaemia cells mediates T cell suppression and tumour infiltration. Nature *562*, 605–609.

20. Knaus, H.A., Berglund, S., Hackl, H., Montiel-Esparza, R., Levis, M.J., Karp, J.E., Gojo, I., and Luznik, L. (2016). Acute myeloid leukemia (AML) blasts influence the gene expression signature and Co-signaling receptor expression of CD8+ T cells. Blood *128*, 1700.

21. Zheng, J., Umikawa, M., Cui, C., Li, J., Chen, X., Zhang, C., Huynh, H., Kang, X., Silvany, R., Wan, X., et al. (2012). Inhibitory receptors bind ANGPTLs and support blood stem cells and leukaemia development. Nature *485*, 656–660.

22. (2013). The genotype-tissue expression (GTEx) project. Nat. Genet. *45*, 580–585.

23. Thorsson, V., Gibbs, D.L., Brown, S.D., Wolf, D., Bortone, D.S., Ou Yang, T.H., Porta-Pardo, E., Gao, G.F., Plaisier, C.L., Eddy, J.A., et al. (2018). The immune landscape of cancer. Immunity *48*, 812–830.e4.

24. Bagaev, A., Kotlov, N., Nomie, K., Svekolkin, V., Gafurov, A., Isaeva, O., Osokin, N., Kozlov, I., Frenkel, F., Gancharova, O., et al. (2021). Conserved pan-cancer microenvironment subtypes predict response to immunotherapy. Cancer Cell *39*, 845–865.e7.

25. Xu, Z.J., Ma, J.C., Zhou, J.D., Wen, X.M., Yao, D.M., Zhang, W., Ji, R.B., Wu, D.H., Tang, L.J., Deng, Z.Q., et al. (2019). Reduced protocadherin17 expression in leukemia stem cells: the clinical and biological effect in acute myeloid leukemia. J. Transl. Med. *17*, 102.

26. Zhao, R., Choi, B.Y., Lee, M.H., Bode, A.M., and Dong, Z. (2016). Implications of genetic and epigenetic alterations of CDKN2A (p16(INK4a)) in cancer. EBioMedicine *8*, 30–39.

27. Sakhdari, A., Tang, Z., Ok, C.Y., Bueso-Ramos, C.E., Medeiros, L.J., and Huh, Y.O. (2019). Homogeneously staining region (hsr) on chromosome 11 is highly specific for KMT2A amplification in acute myeloid leukemia (AML) and myelodysplastic syndrome (MDS). Cancer Genet. *238*, 18–22.

28. Peterson, J.F., Sukov, W.R., Pitel, B.A., Smoley, S.A., Pearce, K.E., Meyer, R.G., Williamson, C.M., Smadbeck, J.B., Vasmatzis, G., Hoppman, N.L., et al. (2019). Acute leukemias harboring KMT2A/MLLT10 fusion: a 10-year experience from a single genomics laboratory. Genes Chromosomes Cancer *58*, 567–577.

29. Dufva, O., Pölönen, P., Brück, O., Keränen, M.A.I., Klievink, J., Mehtonen, J., Huuhtanen, J., Kumar, A., Malani, D., Siitonen, S., et al. (2020). Immunogenomic landscape of hematological malignancies. Cancer Cell *38*, 380–399.e3.

30. Armstrong, S.A., Staunton, J.E., Silverman, L.B., Pieters, R., den Boer, M.L., Minden, M.D., Sallan, S.E., Lander, E.S., Golub, T.R., and Korsmeyer, S.J. (2002). MLL translocations specify a distinct gene expression profile that distinguishes a unique leukemia. Nat. Genet. *30*, 41–47.

31. John, S., Chen, H., Deng, M., Gui, X., Wu, G., Chen, W., Li, Z., Zhang, N., An, Z., and Zhang, C.C. (2018). A novel anti-LILRB4 CAR-T cell for the treatment of monocytic AML. Mol. Ther. *26*, 2487–2495.

32. Hurtz, C., Chan, L.N., Geng, H., Ballabio, E., Xiao, G., Deb, G., Khoury, H., Chen, C.W., Armstrong, S.A., Chen, J., et al. (2019). Rationale for targeting BCL6 in MLL-rearranged acute lymphoblastic leukemia. Genes Dev. *33*, 1265–1279.

33. Akalin, A., Garrett-Bakelman, F.E., Kormaksson, M., Busuttil, J., Zhang, L., Khrebtukova, I., Milne, T.A., Huang, Y., Biswas, D., Hess, J.L., et al. (2012). Base-pair resolution DNA methylation sequencing reveals profoundly divergent epigenetic landscapes in acute myeloid leukemia. PLoS Genet. *8*, e1002781.

34. Su, R., Dong, L., Li, Y., Gao, M., Han, L., Wunderlich, M., Deng, X., Li, H., Huang, Y., Gao, L., et al. (2020). Targeting FTO suppresses cancer stem cell maintenance and immune evasion. Cancer Cell *38*, 79–96.e11.

35. Prange, K.H.M., Mandoli, A., Kuznetsova, T., Wang, S.Y., Sotoca, A.M., Marneth, A.E., van der Reijden, B.A., Stunnenberg, H.G., and Martens, J.H.A. (2017). MLL-AF9 and MLL-AF4 oncofusion proteins bind a distinct enhancer repertoire and target the RUNX1 program in 11q23 acute myeloid leukemia. Oncogene *36*, 3346–3356.

36. De Simone, M., Arrigoni, A., Rossetti, G., Gruarin, P., Ranzani, V., Politano, C., Bonnal, R.J.P., Provasi, E., Sarnicola, M.L., Panzeri, I., et al. (2016). Transcriptional landscape of human tissue lymphocytes unveils uniqueness of tumor-infiltrating T regulatory cells. Immunity *45*, 1135–1147.

37. Liu, X., Yu, X., Xie, J., Zhan, M., Yu, Z., Xie, L., Zeng, H., Zhang, F., Chen, G., Yi, X., et al. (2015). ANGPTL2/LILRB2 signaling promotes the propagation of lung cancer cells. Oncotarget *6*, 21004–21015.

38. Cheng, J., Luan, J., Chen, P., Kuang, X., Jiang, P., Zhang, R., Chen, S., Cheng, F., and Gou, X. (2020). Immunosuppressive receptor LILRB1 acts as a potential regulator in hepatocellular carcinoma by integrating with SHP1. Cancer Biomark *28*, 309–319.

39. Cheng, J., Gao, X., Zhang, X., Guo, H., Chen, S., and Gou, X. (2020). Leukocyte immunoglobulin-like receptor subfamily B member 1 potentially acts as a diagnostic and prognostic target in certain subtypes of adenocarcinoma. Med. Hypotheses *144*, 109863.

40. Barkal, A.A., Weiskopf, K., Kao, K.S., Gordon, S.R., Rosental, B., Yiu, Y.Y., George, B.M., Markovic, M., Ring, N.G., Tsai, J.M., et al. (2018). Engagement of MHC class I by the inhibitory receptor LILRB1 suppresses macrophages and is a target of cancer immunotherapy. Nat. Immunol. *19*, 76–84.

41. Uhl, F.M., Chen, S., O'Sullivan, D., Edwards-Hicks, J., Richter, G., Haring, E., Andrieux, G., Halbach, S., Apostolova, P., Büscher, J., et al. (2020). Metabolic reprogramming of donor T cells enhances graft-versus-leukemia effects in mice and humans. Sci. Transl. Med. *12*.

42. Mussai, F., De Santo, C., Abu-Dayyeh, I., Booth, S., Quek, L., McEwen-Smith, R.M., Qureshi, A., Dazzi, F., Vyas, P., and Cerundolo, V. (2013). Acute myeloid leukemia creates an arginase-dependent immunosuppressive microenvironment. Blood *122*, 749–758.

43. Curti, A., Aluigi, M., Pandolfi, S., Ferri, E., Isidori, A., Salvestrini, V., Durelli, I., Horenstein, A.L., Fiore, F., Massaia, M., et al. (2007). Acute myeloid leukemia cells constitutively express the immunoregulatory enzyme indoleamine 2,3-dioxygenase. Leukemia *21*, 353–355.

44. Tonks, A., Hills, R., White, P., Rosie, B., Mills, K.I., Burnett, A.K., and Darley, R.L. (2007). CD200 as a prognostic factor in acute myeloid leukaemia. Leukemia *21*, 566–568.

45. Li, C., Chen, X., Yu, X., Zhu, Y., Ma, C., Xia, R., Ma, J., Gu, C., Ye, L., and Wu, D. (2014). Tim-3 is highly expressed in T cells in acute myeloid leukemia and associated with clinicopathological prognostic stratification. Int. J. Clin. Exp. Pathol. *7*, 6880–6888.

46. Perna, F., Berman, S.H., Soni, R.K., Mansilla-Soto, J., Eyquem, J., Hamieh, M., Hendrickson, R.C., Brennan, C.W., and Sadelain, M. (2017). Integrating proteomics and transcriptomics for systematic combinatorial chimeric antigen receptor therapy of AML. Cancer Cell *32*, 506–519.e5.

47. Xu-Monette, Z.Y., Li, L., Byrd, J.C., Jabbar, K.J., Manyam, G.C., Maria de Winde, C., van den Brand, M., Tzankov, A., Visco, C., Wang, J., et al. (2016). Assessment of CD37 B-cell antigen and cell of origin significantly improves risk prediction in diffuse large B-cell lymphoma. Blood *128*, 3083–3100.

48. Schetters, S.T.T., Rodriguez, E., Kruijssen, L.J.W., Crommentuijn, M.H.W., Boon, L., Van den Bossche, J., Den Haan, J.M.M., and Van Kooyk, Y. (2020). Monocyte-derived APCs are central to the response of PD1 checkpoint blockade and provide a therapeutic target for combination therapy. J. Immunother. Cancer *8*. e000588.

49. Chen, H.M., van der Touw, W., Wang, Y.S., Kang, K., Mai, S., Zhang, J., Alsina-Beauchamp, D., Duty, J.A., Mungamuri, S.K., Zhang, B., et al. (2018). Blocking immunoinhibitory receptor LILRB2 reprograms tumor-associated myeloid cells and promotes antitumor immunity. J. Clin. Invest. *128*, 5647–5662.

50. Consortium, G. (2013). The genotype-tissue expression (GTEx) project. Nat. Genet. *45*, 580–585.

51. Ritchie, M.E., Phipson, B., Wu, D., Hu, Y., Law, C.W., Shi, W., and Smyth, G.K. (2015). Limma powers differential expression analyses for RNA-sequencing and microarray studies. Nucleic Acids Res. *43*, e47.

52. Camp, R.L., Dolled-Filhart, M., and Rimm, D.L. (2004). X-tile: a new bio-informatics tool for biomarker assessment and outcome-based cut-point optimization. Clin. Cancer Res. *10*, 7252–7259.

53. Tamborero, D., Rubio-Perez, C., Muiños, F., Sabarinathan, R., Piulats, J.M., Muntasell, A., Dienstmann, R., Lopez-Bigas, N., and Gonzalez-Perez, A. (2018). A pan-cancer landscape of interactions between solid tumors and infiltrating immune cell populations. Clin. Cancer Res. *24*, 3717–3728.

54. Sturm, G., Finotello, F., Petitprez, F., Zhang, J.D., Baumbach, J., Fridman, W.H., List, M., and Aneichyk, T. (2019). Comprehensive evaluation of transcriptome-based cell-type quantification methods for immuno-oncology. Bioinformatics *35*, i436–i445.